ANTENNA RECONFIGURATION USING ELECTRICALLY ACTUATED LIQUID-METAL PIXELS

A THESIS SUBMITTED TO THE GRADUATE DIVISION OF THE UNIVERSITY OF HAWAIʻI AT MĀNOA IN PARTIAL FULFILLMENT OF THE REQUIREMENTS FOR THE DEGREE OF

MASTER OF SCIENCE

IN

ELECTRICAL ENGINEERING

DECEMBER 2017

By

Kent J. Sarabia

Thesis Committee:

Wayne Shiroma, Chairperson
Aaron Ohta
Olga Boric-Lubecke

ACKNOWLEDGMENTS

This research has been made possible with the guidance, and patience, of Dr. Wayne Shiroma, Dr. Aaron Ohta, and the colleagues met at the University of Hawai‘i at Mānoa (UHM). This research has been supported by the Defense Advanced Research Projects Agency (DARPA) under Grant W31P4Q-16-1-0005.

Thank you!

ABSTRACT

Reconfigurable antennas provide a versatile solution to current demands in wireless communications, where multiple frequency bands are in use. Such antennas can change their properties, such as operational frequency, in response to a dynamic environment. This allows for cost-effective wireless communications systems which would otherwise require a dedicated antenna for every operational frequency band. This thesis presents a technique to realize a frequency-reconfigurable antenna using discrete amounts of electrically actuated liquid metal. The liquid metal functions as a pixel which, when made in an array, can create discrete conductive 2-D structures to use as an antenna.

Table of Contents

Tables

Figures

Chapter 1

Introduction

Wireless communication is an integral part of modern society. From cellular phones in our hands to satellites in space, antennas are in use everywhere. A problem in wireless communications is having too many antennas. Systems that operate at a wide range of frequencies will often employ multiple antennas which are complex, bulky, and ultimately costly. An example is in a smartphone [1] that is equipped to access the internet either by WiFi or using an LTE network. The smartphone has an antenna dedicated to communicating at WiFi frequencies and another antenna dedicated to the LTE network.

Reconfigurable antennas offer an adaptive solution in a dynamic communication environment, demonstrating the ability to change radiation pattern, polarization, and operational frequency [2, 3]. Returning to the smartphone example, a smartphone can replace antennas used for WiFi and LTE frequencies with a reconfigurable antenna. The reconfigurable antenna replaces two or more antennas used for an application, like internet, with a versatile antenna that changes according to the user's needs. A frugal college student would enjoy the reconfigurable antenna actively changing into a WiFi antenna when a hotspot is available. Although reconfigurability is typically achieved using PIN diodes [4], varactors [5], or MEMS switches [6], liquid metal has also recently been shown to implement reconfigurable antennas. Recent demonstrations in liquid-metal reconfigurable antennas include monopole [7, 8] dipole [9], planar inverted F [10], Yagi-Uda [11, 12, 13], patch [14, 15], and slot [16] antennas.

Reconfigurability is achieved either by altering the physical dimensions of the radiating element with liquid metal, or by configuring an associated liquid-metal parasitic element.

This thesis presents reconfiguration by changing the dimensions of an antenna with discretized pixels of liquid metal. This approach, known as pixelation, realizes what is called a pixelated antenna which have been demonstrated by connecting solid metal conductors with switches [17, 18]. By connecting the solid metal conductors to create a desired structure, a pixelated antenna can realize an optimized 2-D structure for a specific antenna need.

However, this approach does not come without problems. This approach typically requires an interconnecting switch between adjacent pixels; for an $N \times N$ pixel array, the number of switches needed is $2N(N-1)$. As the number of pixels N increases, so does the corresponding complexity in control circuitry and increased insertion loss. Typical switches used in pixelated antennas utilize PIN diodes, MEMS switches, or FET switches. In an optimized case 30 PIN diodes consume 0.42 W of power, with each PIN diode drawing 20 mA [18]. Another problem with using switches is the impact it has on antenna efficiency. Efficiencies of 40% - 50% have been reported due PIN diode losses [18].

This thesis presents research in solving this problem with liquid metal. Instead of connecting discretized metal with a switch, discretized liquid metal will be electrically actuated into place to create the desired 2-D structure through continuous electrowetting (CEW) [19]. This removes the need for a switch between each pixel and instead requires a circuit for each individual pixel. This reduces the total number of required switches from $2N(N-1)$ to $N \times N$, reducing complexity and cost. Liquid-metal actuation using CEW is low power, with power consumption reported at 10 μW to operate [19]. In addition, the power requirements are only to move the liquid metal. Once liquid metal is actuated into place, the CEW electrical signal needed

to move the liquid metal is no longer needed. This is a significant advantage over PIN diodes, where a constant bias is required.

Chapter 2 presents out-of-plane actuating of liquid metal where the ability to actuate liquid metal against the force of gravity is investigated. Chapter 3 applies the findings of Chapter 2 to develop a liquid-metal pixel. Finally, Chapter 4 applies the liquid-metal pixel to a dipole antenna to demonstrate frequency reconfiguration.

Chapter 2

Out-of-plane continuous electrowetting actuation of liquid metal[1]

Liquid-metal-based circuits have recently emerged as an innovative electronics technology for realizing flexible sensors [20], stretchable electronics [21], and reconfigurable devices [22, 23]. In these types of applications, the possibility of manipulating a room-temperature liquid metal into a desired shape opens up a wide breadth of flexible applications.

Although mechanical pumps are often the easiest method of actuating liquid-metal devices, they are not quite compatible with integrated-circuit technology. Such compatibility is achieved with electrical actuation methods such as electrocapillary actuation [24] and continuous electrowetting (CEW) [19]. As developments in liquid-metal-based circuits continue to mature, one can imagine the possibility of highly integrated, multi-layer microfluidic lab-on-a-chip technology.

With few exceptions [25], most liquid-metal circuits are limited to two-dimensional, in-plane movement of the liquid metal. This chapter demonstrates the first three-dimensional, out-

[1] The work presented in this chapter is based on: K. J. Sarabia, S. S. Yamada, R. C. Gough, M. R. Moorefield, A. W. Combs, W. A. Shiroma, and A. T. Ohta, "Out-of-plane continuous electrowetting of liquid metal," *Electron. Lett.,* vol. 53, no. 25, pp. 1635–1636, 7 Dec. 2017.

of-plane motion of liquid metal. CEW is used to provide sufficient actuation force on the liquid metal to move it against the force of gravity.

2.1 Device design

To demonstrate the out-of-plane actuation of liquid metal, a prototype was fabricated that electrically actuates liquid metal from one reservoir to another located at a higher elevation. The device, shown in Figure 2.1, consists of three reservoirs on a 1.57-mm-thick Rogers RT Duroid 5880 substrate. The walls and ceiling of Reservoirs 1 and 2 are made of polydimethylsiloxane (PDMS). A layer of polyimide forms the floor of Reservoirs 1 and 2. Reservoirs 1 and 3 are connected by a channel through the substrate that is used to move the liquid metal between these two reservoirs. A smaller channel connects Reservoirs 2 and 3 and serves as an electrical path for the actuation signal. The entire device is filled with a 5% weight-per-volume concentration of sodium hydroxide solution (NaOH). Galinstan [26], a eutectic liquid-metal alloy that consists of gallium, indium, and tin, is injected to fill Reservoir 1. The liquid metal ideally moves between Reservoirs 1 and 3, depending upon on the polarity of an applied voltage; the liquid metal moves toward the positive electrode.

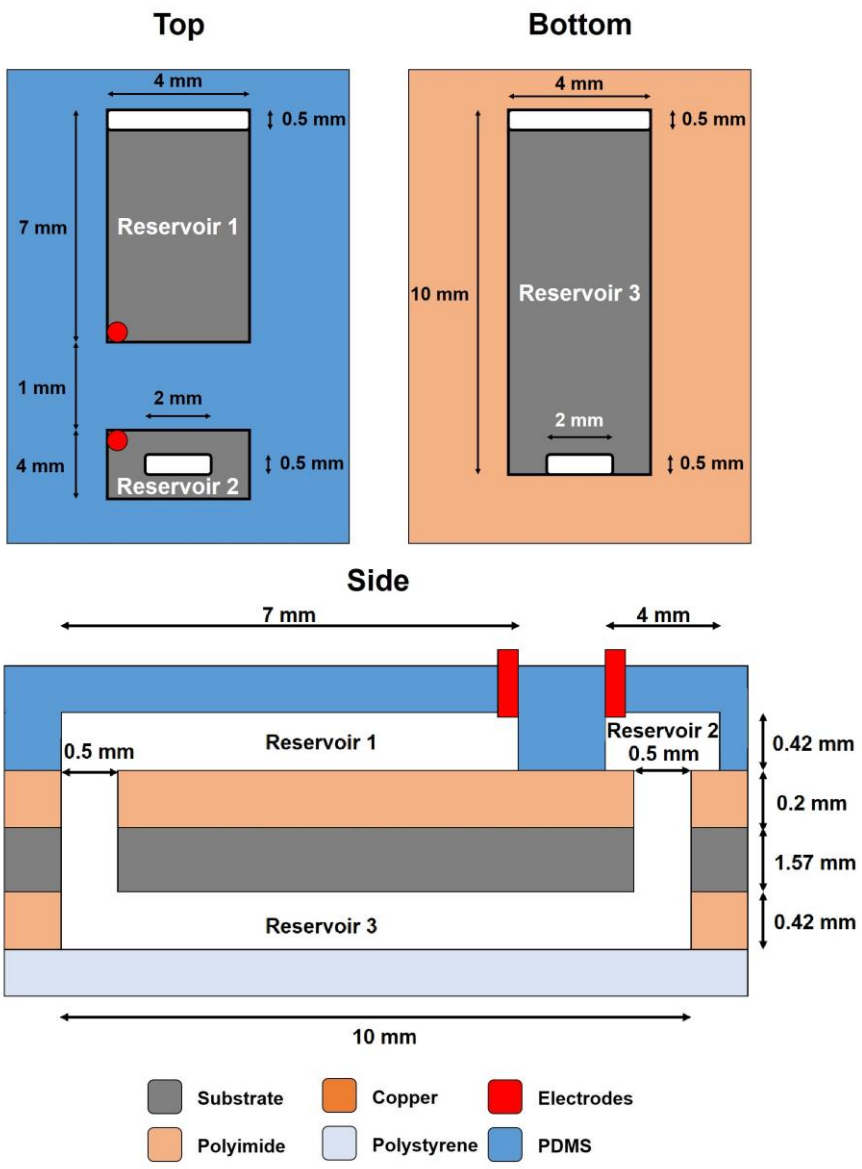

Figure 2.1: Layout of out-of-plane actuation the device. Liquid metal moves between Reservoirs 1 and 3 when a voltage is applied to the electrodes.

2.2 Experimental Results

An electrical signal was applied to the electrodes to actuate the liquid metal. The signal was an 8 V-pp square wave with a +3 V DC offset at 50% duty cycle. The slug actuates 11 mm

from the end of Reservoir 3 to Reservoir 1, shown in Figures 2.2 and 2.3. This demonstrates actuation opposing the force of gravity, which exerts a force of 0.74 mN on the liquid-metal slug. The speed at which the slug moves varies by direction. The slug takes approximately 1 s to actuate down, with the aid of gravity. The time to actuate increases to 1.66 s when the slug actuates against the force of gravity. This was observed with a camera at 30 frames per second (fps).

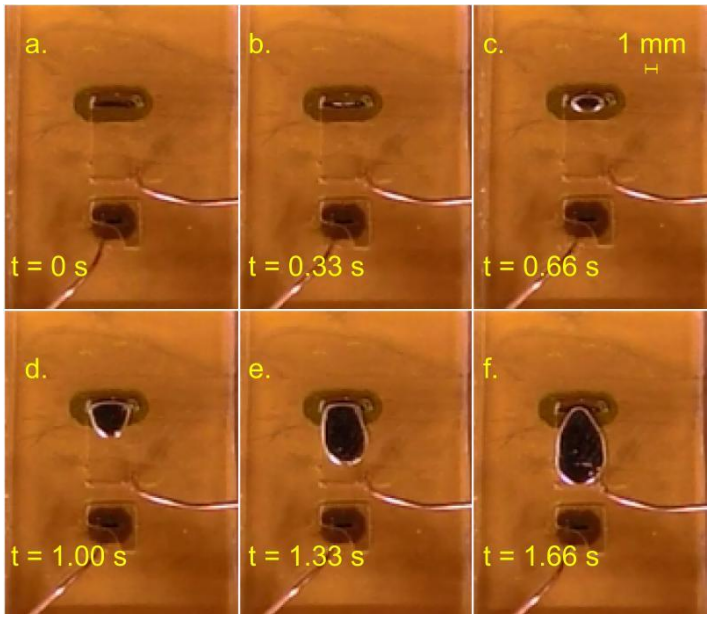

Figure 2.2: Out-of-plane actuation of liquid metal. (a) The actuation voltage is applied. (b) to (e) Liquid metal moves from a reservoir beneath the surface shown here, into a reservoir on the surface. (f) Completed actuation of the liquid metal. Observed with a 30-fps camera.

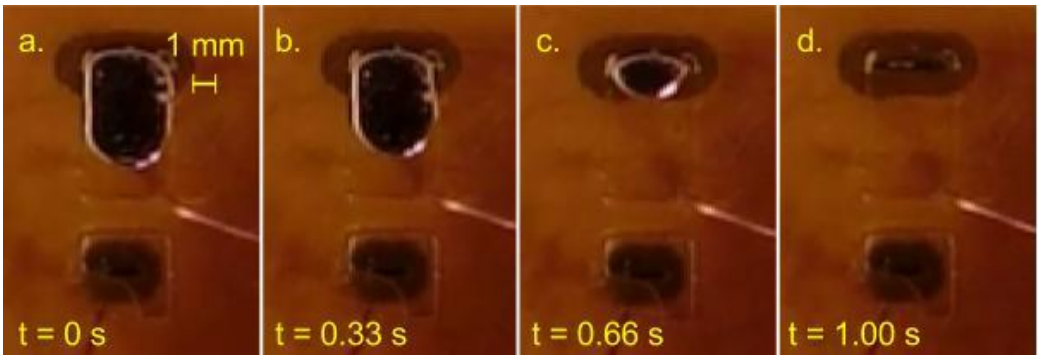

Figure 2.3: Out-of-plane actuation of liquid metal to a reservoir beneath the surface. (a) The actuation voltage is applied. (b) and (c) Liquid metal moves to reservoir below. (d) Completed actuation of the liquid metal. Observed with a 30-fps camera.

The device demonstrates that electrical actuation of liquid metal opposing the force of gravity is possible. An analysis of the actuation mechanism will be discussed in the next section.

2.3 Discussion

The liquid-metal actuation mechanism is continuous electrowetting (CEW). This requires liquid metal to be submerged in an electrolyte solution. An electrical double layer (EDL) forms at the interface of the metal and solution [19]. The EDL can be manipulated with the application of a voltage potential, as described by the Young-Lippman equation:

$$\gamma = \gamma_0 - \frac{C}{2}(V - V_0)^2, \tag{2.1}$$

where γ is the surface tension of the liquid metal, γ_0 is the intrinsic surface tension of the liquid metal, C is the capacitance per unit area across the EDL, V_0 is the intrinsic voltage across the EDL, and V is an externally applied voltage across the EDL. When a potential is applied to the liquid metal, an imbalance of charge changes the surface tension on one side of the liquid metal. This creates a pressure differential as described by the Young-Laplace equation [6]:

$$\rho = \gamma\left(\frac{1}{a}+\frac{1}{b}\right), \tag{2.2}$$

where ρ is the pressure differential, γ is the surface tension, and a and b are the radii of curvature of the liquid metal. The force generated on the liquid metal is approximately this pressure differential multiplied by the cross-sectional area of the channel surrounding the liquid metal.

Experimental results have shown that an applied voltage generates enough force to move a slug of Galinstan, which has a density of 6440 kg/m^3 [26], against the force of gravity. The liquid-metal slug used in these experiments is 7 mm long in a channel with a cross section of 4 mm × 0.42 mm, and has a mass of 0.076 g. Gravity exerts a force of 0.74 mN on the slug.

Using channel dimensions of the device described here, a surface tension γ was calculated using (2.2) by assuming a pressure that yields a force equal to that of gravity. The applied voltage necessary to achieve this surface tension was then calculated using (2.1). It was found that a voltage greater than 3.18 V will generate a CEW force that can overcome the force of gravity for a liquid-metal slug with the dimensions mentioned above. In the experiments described here, an 8-V signal was applied to the electrodes. The voltage difference across the

liquid-metal slug is lower than the voltage across the electrodes due to the voltage drop across the electrolyte [19]. However, the voltage across the liquid-metal slug is greater than 3.18 V, resulting in out-of-plane actuation.

2.4 Summary

By repeatedly moving a liquid-metal slug from one reservoir to another placed at a higher elevation, this chapter demonstrated the out-of-plane CEW actuation of Galinstan liquid metal against the force of gravity. This demonstrates the viability of electrical actuation of liquid metal in three dimensions.

Chapter 3

Pixelated reconfiguration using electrically actuated liquid metal[2]

A reconfigurable antenna is an important element in an adaptive wireless system, capable of adjusting its operating parameters such as resonant frequency, radiation pattern, and polarization to meet varying needs [27]. One reconfiguration technique is pixelation, in which discrete conductive pixels are used as the radiator [17] or reconfigurable parasitic load [18]. This approach typically requires an interconnecting switch between adjacent pixels; for an $N \times N$ pixel array, the number of switches needed is $2N(N-1)$. As the number of pixels N increases, so does the corresponding complexity in control circuitry and increased insertion loss.

This chapter presents a two-dimensional pixelation technique that does not require any switches to connect and disconnect adjacent pixels. Instead, pixels either appear or disappear, using one activation circuit per pixel that fills with liquid metal to make it appear, or evacuates to make it disappear. This results in a reduction from $2N(N-1)$ switches to N^2 activation circuits, as shown in Figure 3.1.

[2] The work presented in this chapter is based on: K. J. Sarabia, W. A. Shiroma, and A. T. Ohta, "Pixelated reconfiguration using electrically actuated liquid metal," *Electron. Lett.,* submitted Nov. 2017.

A wide variety of reconfigurable RF circuits have already been designed using liquid metal [7, 8, 28–31]. This chapter reports the first two-dimensional liquid-metal pixel array that could serve as the basis for a pixelated antenna.

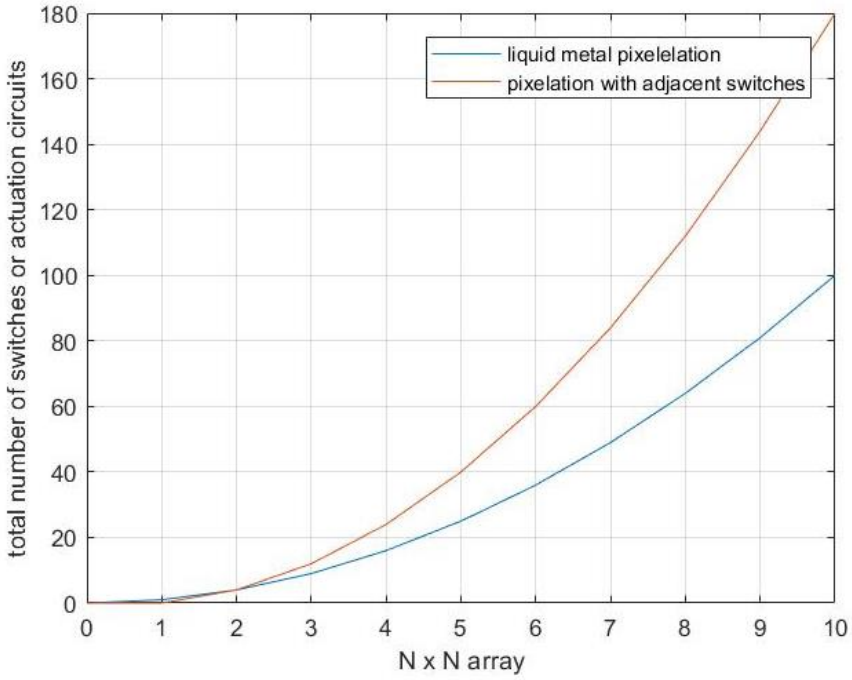

Figure 3.1: Number of actuation circuits vs. switches needed in a pixelated $N \times N$ surface.

3.1 Pixel grid layout

To demonstrate the concept, Figure 3.2 shows a prototype 2 × 2 liquid-metal grid. Each pixel employs a recently developed, three-dimensional, out-of-plane actuation technique for moving Galinstan liquid metal [32]. Figure 3.2a shows the pixelated surface on one side of the supporting substrate, with adjacent pixels joined by stainless-steel connectors embedded in the

walls separating each pixel. Figure 3.2b shows the opposite side of the substrate that houses the actuation circuit consisting of two electrodes placed in each pixel. Electrode 1 extends through the substrate to reservoir 1, with polyimide insulating it from reservoir 2 (Figure 3.2c). Stainless-steel syringes are punctured into reservoir 2 to serve as electrodes.

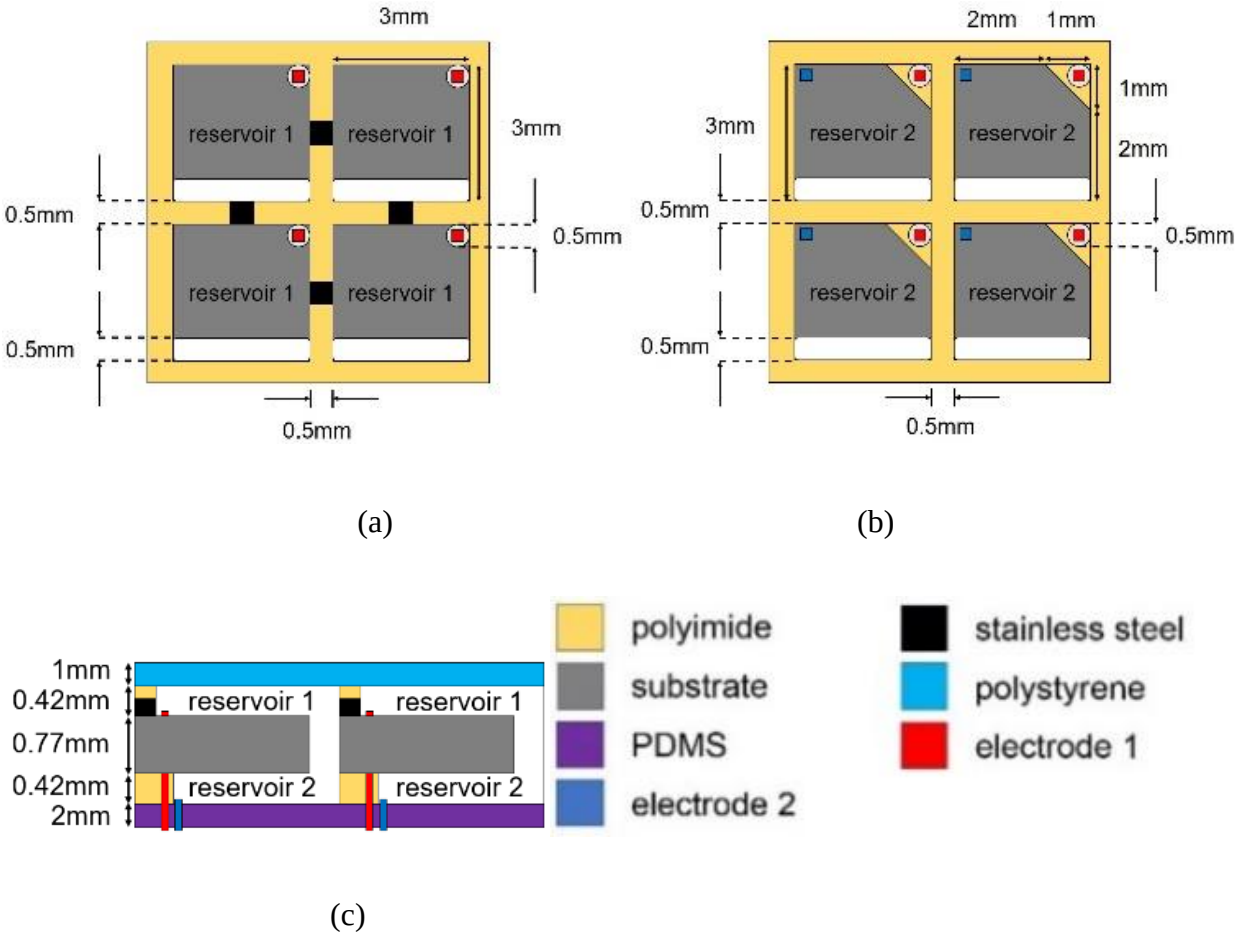

Figure 3.2: Layout of 2 × 2 grid. (a) Top side containing reservoir 1 pixels. (b) Bottom side containing reservoir 2 pixels. (c) Cross-sectional view of grid.

3.2 Liquid-metal actuation

Figure 3.3 illustrates the sequence of steps to actuate liquid metal from reservoir 2 to reservoir 1. Each pixel is flooded with a 1-M concentration of sodium hydroxide (NaOH). Actuation is based on continuous electrowetting (CEW), in which an electrical double layer (EDL) forms at the interface of the liquid metal and NaOH [19]. Applying a voltage to the EDL causes a charge imbalance that creates a pressure differential, which in turn actuates the liquid metal residing in reservoir 2 to reservoir 1.

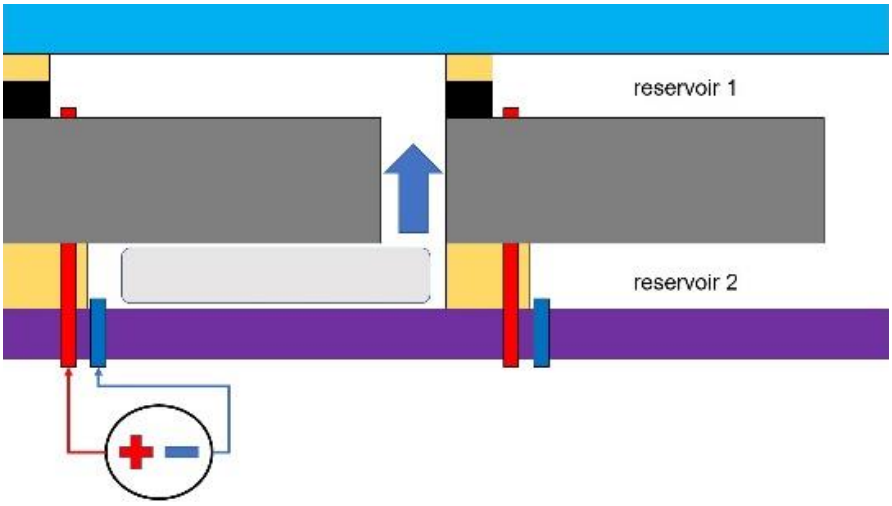

(a)

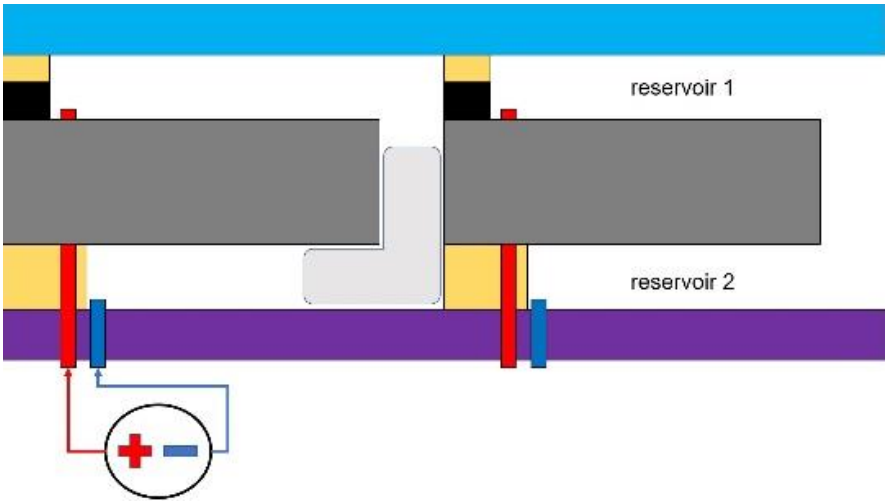

(b)

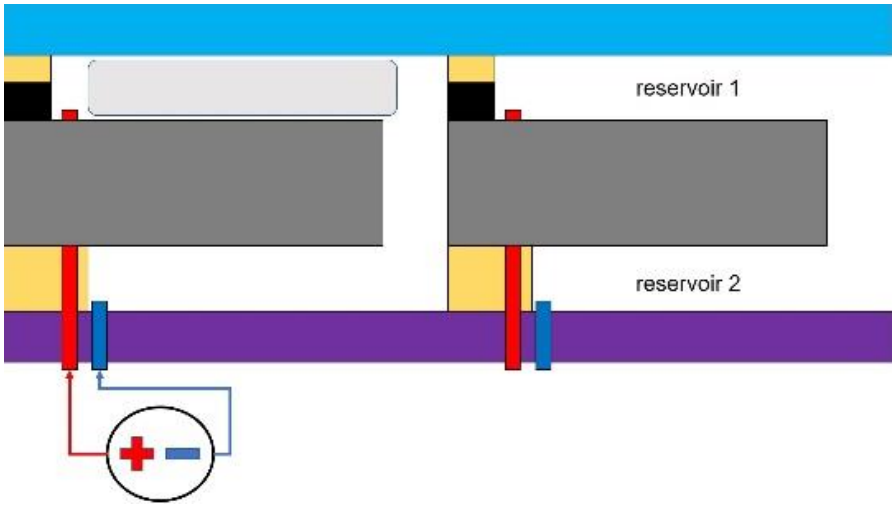

(c)

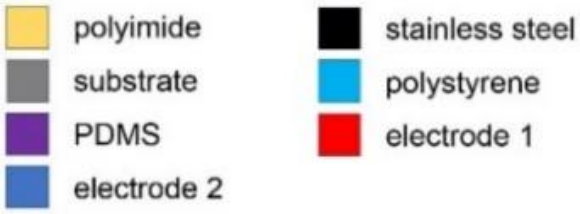

Figure 3.3: Illustration of actuation mechanism in a pixel. (a) Application of actuation voltage on liquid metal. CEW moves liquid metal from reservoir 2 to reservoir 1. (b) Liquid metal starts to move to reservoir 1. (c) Actuation of liquid metal is completed.

3.3 Experimental results

To actuate the liquid metal, a 30-Hz 4-V square wave with a +1 V DC offset is applied to the pixel electrodes. The actuated liquid metal contacts the stainless-steel connectors embedded between pixels, creating an electrical path to adjacent pixels. To return the liquid metal to reservoir 2, the actuation voltage polarity on the electrodes is reversed. Once the voltage is applied, the liquid metal detaches from the stainless steel and retreats to reservoir 2. Figure 3.4 shows that liquid metal actuates between reservoirs within 0.3 s. The filling and evacuating of each pixel is repeatable as long as there is NaOH in each pair of reservoirs. Each pixel can be individually controlled to create any permutation of the 2 × 2 grid.

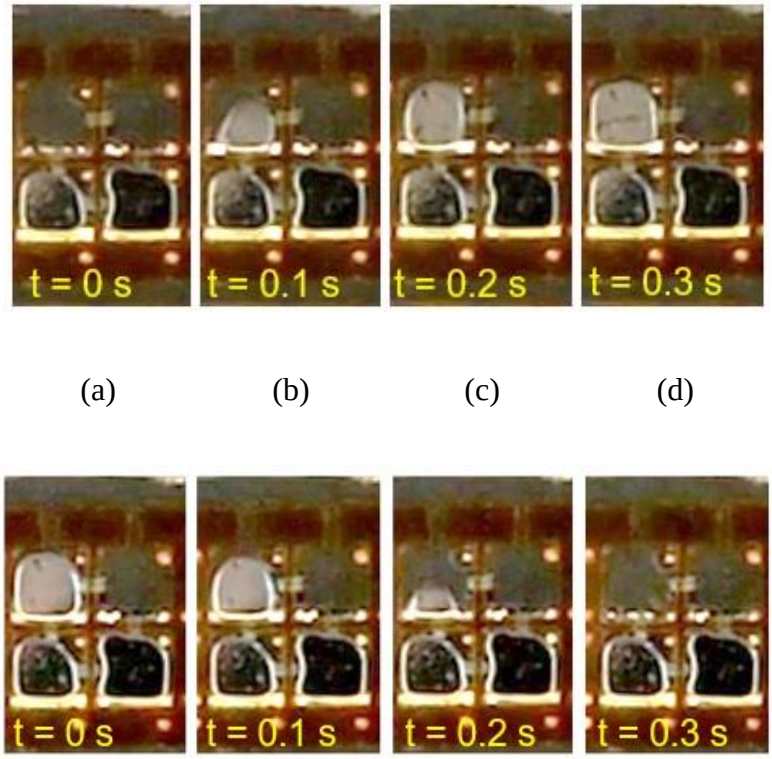

Figure 3.4: Actuation of liquid metal in grid (a) Actuation voltage is applied to the electrodes in top left pixel. (b)–(c) Liquid metal actuates from reservoir 2 and interfaces with stainless steel in the pixel walls. (d) Liquid-metal actuation is completed in 0.3 s and actuation voltage is removed. (e) Voltage applied to electrodes is swapped to change direction of actuation. (f)–(g) Liquid metal actuates back to the reservoir 2. (h) Liquid metal actuation is completed in 0.3 s and the actuation voltage is removed. Observed with a 30 fps camera.

3.4 Summary

Liquid metal in a 2 × 2-pixel grid is electrically actuated, demonstrating pixelated reconfiguration. CEW is used to actuate the liquid metal by applying a 4-V square wave with a

+1 V DC offset to electrodes within the pixels. The liquid metal in each pixel can move to a reservoir buried beneath the grid. The pixels can reversibly switch between on and off states within 0.3 s.

Chapter 4

Frequency-reconfigurable dipole antenna using liquid-metal pixels[3]

This chapter achieves frequency reconfiguration using liquid metal in the form of square pixels. Pixelated antennas have been demonstrated before [17, 18, 33, 34], but this chapter presents a novel method to implement antenna pixelation using liquid metal. To turn on a pixel, a discrete amount of liquid metal is electrically actuated from a reservoir buried below the antenna. To turn off a pixel, the liquid metal retreats to the buried reservoir [31].

4.1 Liquid-Metal Pixelated Dipole

The resonant frequency of a half-wavelength dipole antenna depends on the electrical length of the dipole arms. Using liquid-metal pixels to adjust the dipole length results in discrete changes in the antenna's operating frequency. Figure 4.1 illustrates the concept. The liquid-metal pixelated antenna is based on the dimensions of a 64-mm-long baseline planar copper dipole on a 0.787-mm-thick Duroid 5880 substrate, shown in Figure 4.1(a). The liquid-metal pixelated

[3] The work presented in this chapter is based on: K. J. Sarabia, S. S. Yamada, R. C. Gough, M. R. Moorefield, A. W. Combs, A. T. Ohta, and W. A. Shiroma, "Frequency-reconfigurable dipole antenna using liquid-metal pixels," *Int. J. Antennas Propag.,* submitted Oct. 2017.

antenna shown in Figure 4.1(b) replaces a section of both dipole arms with a 1 × 4 pixel array. The walls of the pixel array are made of polyimide. The top side of the array is covered in polystyrene and the bottom side of the array is covered in polydimethylsiloxane (PDMS). Adjacent pixels on the top side are interconnected with stainless-steel connectors embedded between the pixel walls. The pixel array connects to the copper section of the antenna through a soldered stainless-steel wire. This is necessary as gallium-based liquid metals such as the Galinstan [26] used in this antenna amalgamates to copper, compromising actuation. The interface between the copper and pixel array is covered in a water-tight polymer which is not shown in Figure 4.1.

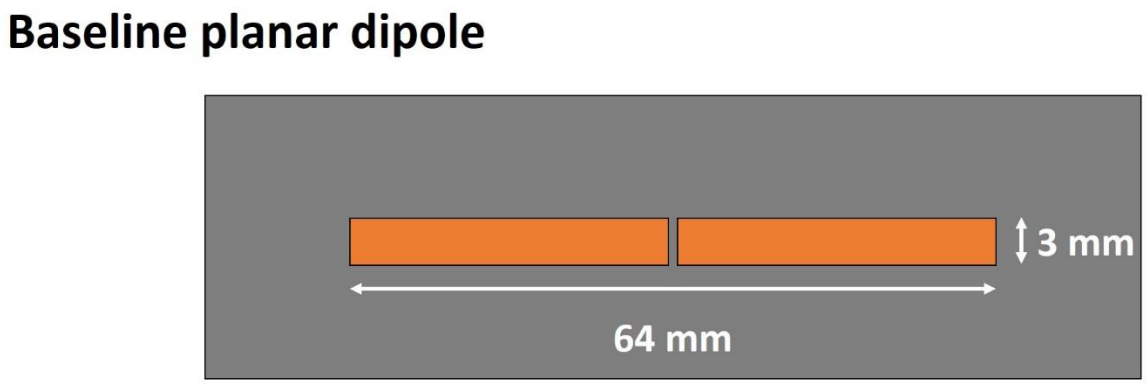

(a)

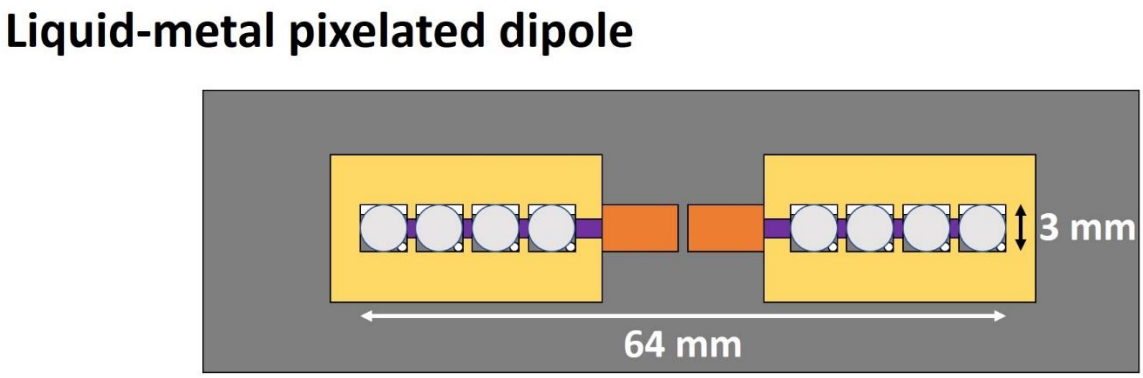
Liquid-metal pixelated dipole
3 mm
64 mm

(b)

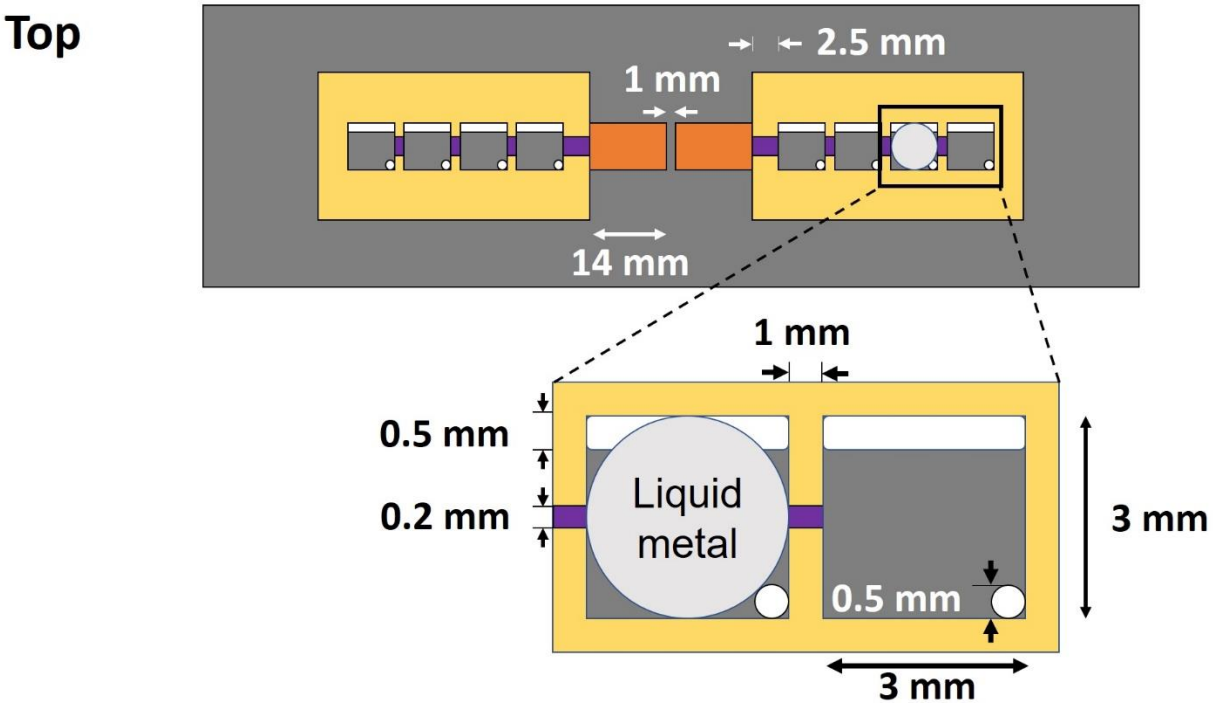
Top
2.5 mm
1 mm
14 mm
1 mm
0.5 mm
0.2 mm
Liquid metal
0.5 mm
3 mm
3 mm

(c)

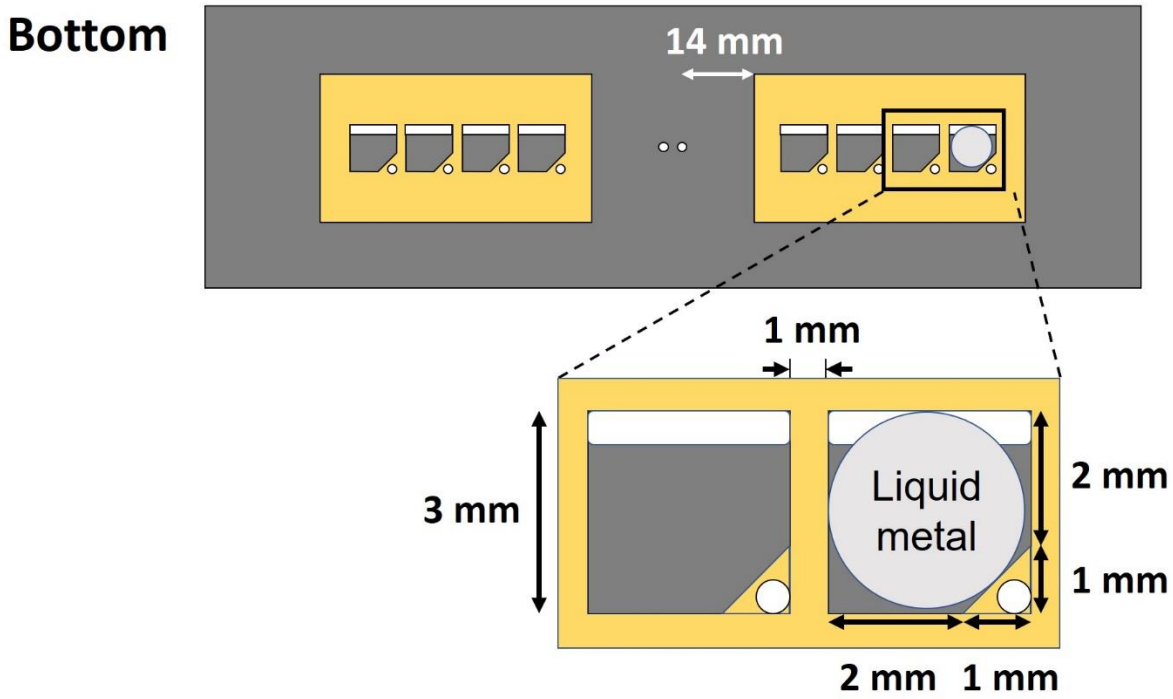

(d)

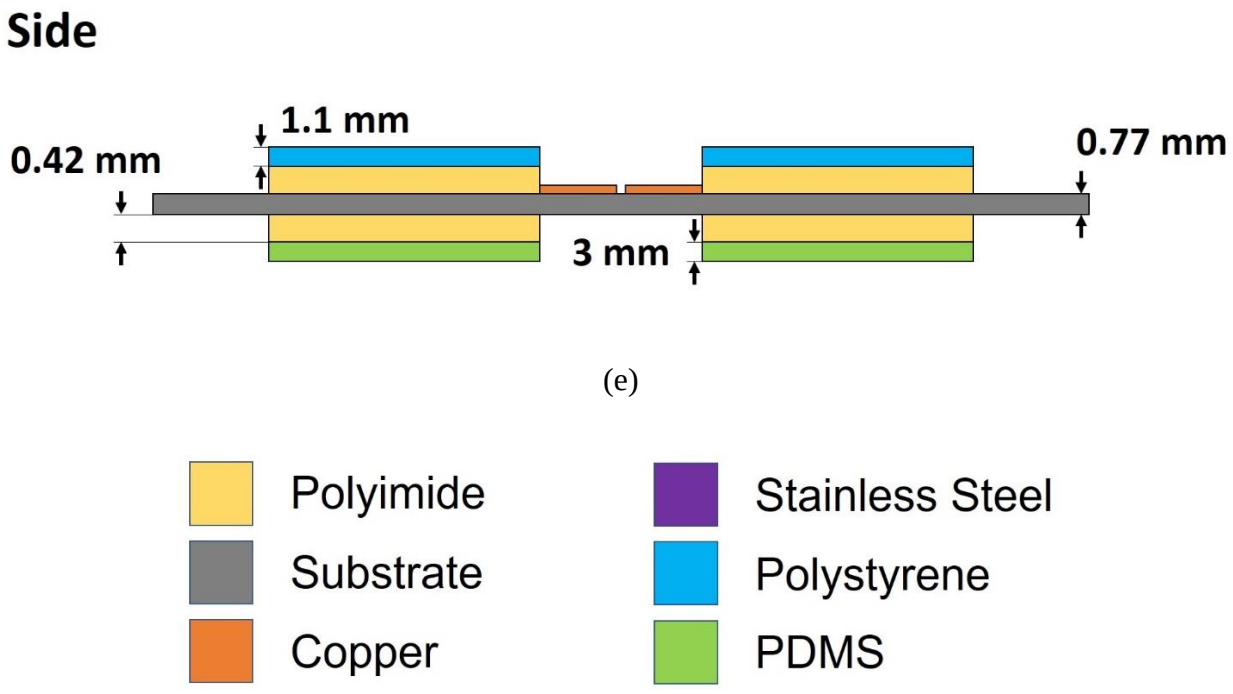

(e)

Figure 4.1: Layout of prototype pixelated liquid-metal dipole antenna. (a) Baseline planar dipole antenna to compare to liquid-metal pixelated equivalent. (b) Liquid-metal pixelated dipole

prototype filled with liquid metal. (c) Top side with zoom-in of pixels. The left pixel is in the ‘on’ state, with liquid metal present and interfacing with stainless steel placed within the walls between pixels. (d) Bottom side with zoom-in of pixels. The right pixel is in the ‘off’ state. (e) Side view.

4.2 Liquid-Metal Pixel

A layout of a pixel is shown in Figure 4.2. Liquid metal moves between the top and bottom reservoirs by applying a voltage on the electrodes. Both electrodes are fed through the bottom reservoir which is covered with a layer of PDMS. The electrodes are electrically isolated from each other on the bottom side of the pixel. A pixel is considered ‘on’ when the liquid metal is actuated to the top-side reservoir of the antenna. The pixel is turned ‘off’ when the liquid metal is actuated to the bottom-side reservoir.

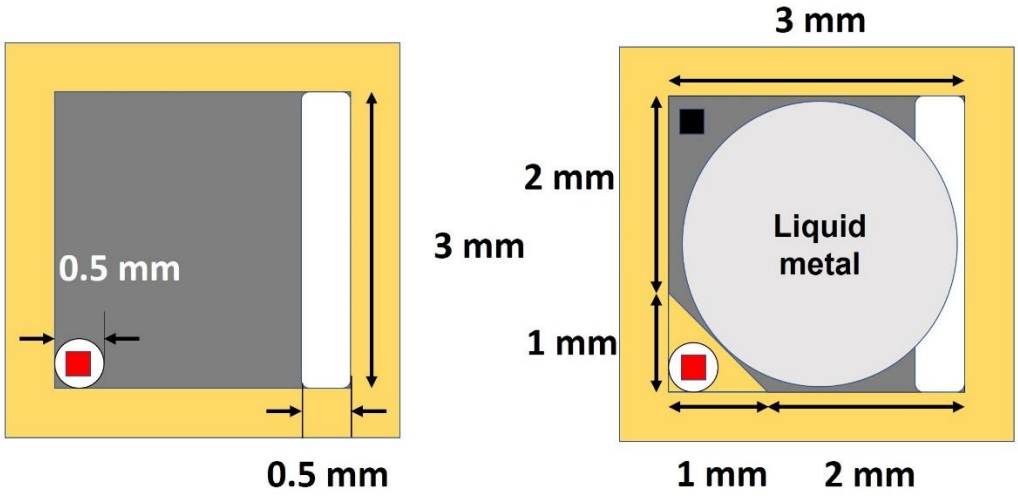

(a) (b)

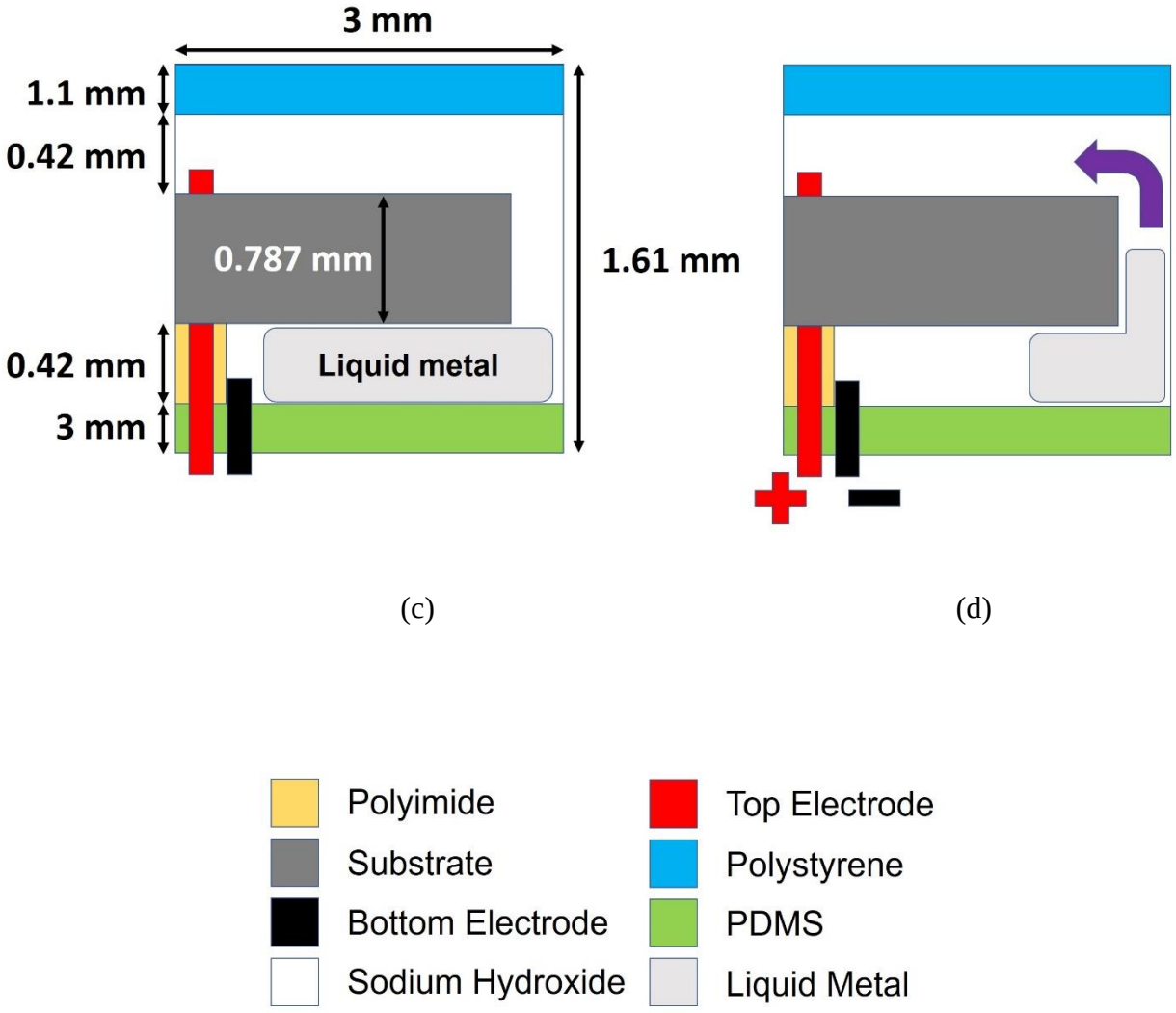

Figure 4.2: Layout of pixel in the 'off' state. (a) Top side of pixel (b) Bottom side with liquid metal present. (c) Side view with liquid metal residing in the bottom side. (d) Application of voltage on the electrodes moves the liquid metal from the bottom side to the top side.

4.3 Liquid Metal Actuation Mechanism

Liquid metal is actuated by manipulating its surface tension using continuous electrowetting (CEW) [19]. Liquid metal is immersed in a 1-M solution of sodium hydroxide

(NaOH), forming an electrical double layer (EDL) at the metal-NaOH interface. A voltage acting on the EDL creates a surface tension imbalance on the liquid metal. This results in a pressure differential, actuating the liquid metal. Figure 4.3 demonstrates actuation in an early 4-mm-square liquid-metal pixel prototype. A 1.2-V square wave with a +1-V DC offset is applied to the electrodes to actuate the liquid metal from a reservoir buried below. The liquid metal is then actuated back to the reservoir by swapping the applied voltage polarities on the electrodes.

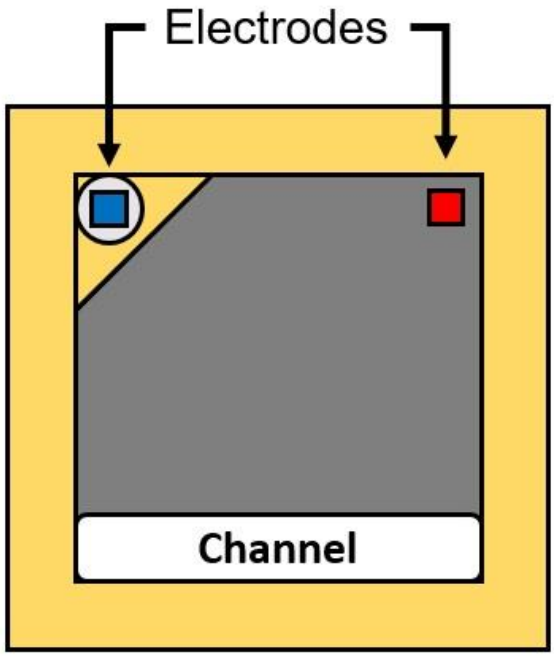

(c)

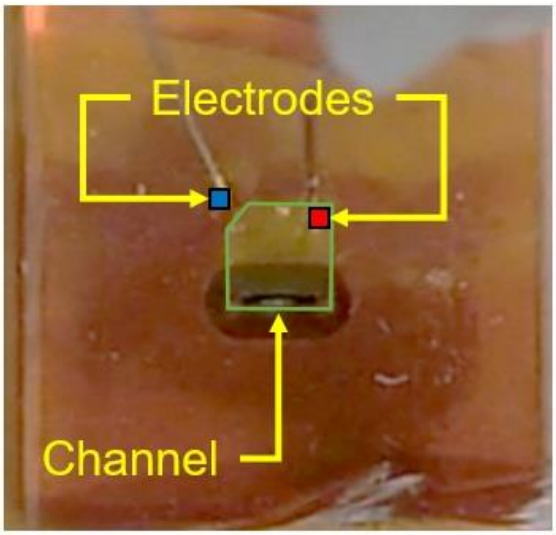

(d)

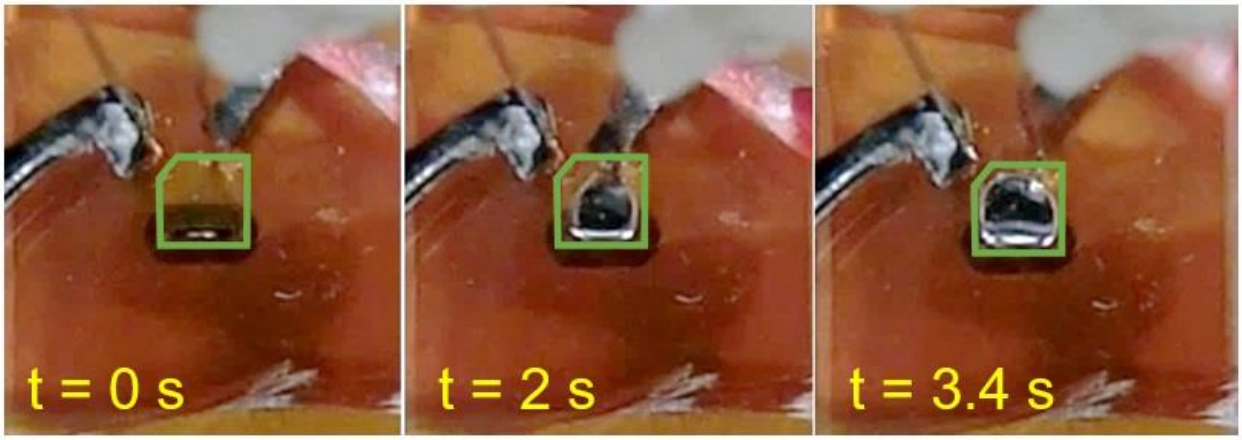

(c) (d) (e)

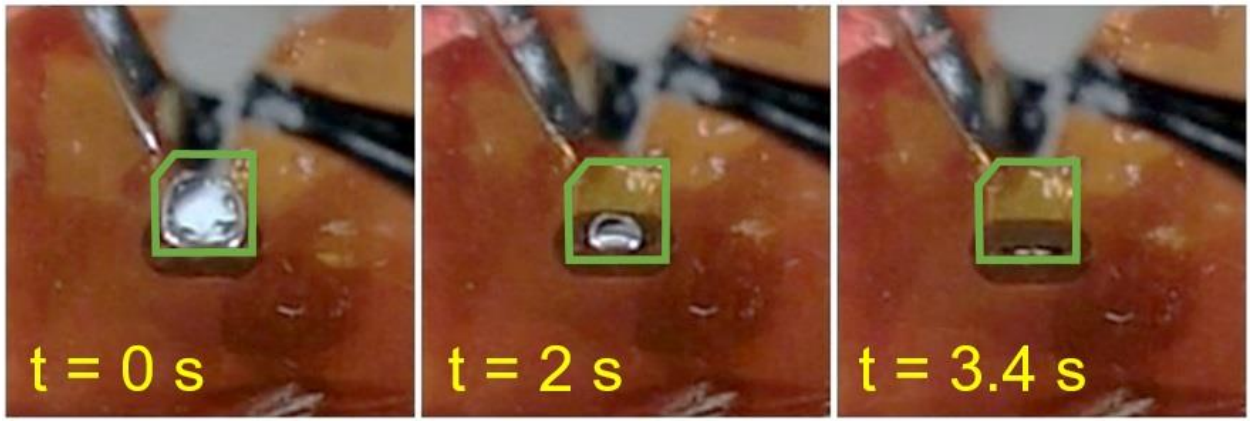

(f) (g) (h)

Figure 4.3: Actuation of liquid metal in a pixel (a) Layout of the prototype pixel bottom side with actuation circuit. (b) Fabricated pixel with outlined pixel and electrodes. Stainless-steel syringes (not shown) are used to puncture the PDMS. (c) Application of 1.2 V to actuate liquid metal from reservoir buried below. (d) Liquid metal actuating. (e) Completion of liquid metal actuation. (f) Swapping voltage applied to electrodes. (g) Liquid metal retreats to reservoir below. (h) Completion of liquid-metal actuation. Observed with a 30-fps camera.

The pixels built for the liquid-metal pixelated dipole utilize a 3-mm-square design. The actuation voltage for this design is a 30-Hz 4-V square wave with a +1-DC offset, which induces a larger actuation force than the 1.2-V actuation voltage used in the 4-mm-square prototype pixel. The larger force acting on a smaller body of liquid metal within the pixel significantly increases actuation speeds, being able to switch the pixel between the on and off states within 0.03 to 0.09 seconds. In comparison to switch-based pixelated antennas, the pixels change states slower. PIN diode and MEMS switches take microseconds, with FET switches requiring nanoseconds to change states.

4.4 Experimental Results

The antenna is tested by incrementally turning on one pixel on each dipole arm and then measuring the resulting resonance frequency and radiation pattern. Figure 4.4 shows measured and simulated frequencies of the antenna with 1–4 pixels active on each dipole arm. Mismatch is expected at higher frequencies due to a combination of the antenna being fed with an SMA connector and utilization of a 50-Ω coaxial cable to match a dipole's typical 73-Ω impedance. Measured and simulated data share a similar trend where higher-frequency states are not well matched, however measured results show that the magnitude of mismatch across all states is better than simulated. The measured resonance frequencies agree with simulated values obtained from an ANSYS HFSS model shown in Table 4.1. As expected, lengthening the dipole by adding liquid-metal pixels in each arm decreases the resonant frequency of the antenna. As the antenna becomes longer, the incremental frequency shift decreases as the inverse square of the antenna length, as expected from the derivative of $f = v / \lambda = v / 2l$:

$$\frac{df}{dl} = -\frac{v}{2l^2}, \tag{3.1}$$

where f is frequency, l is antenna length, and v is the propagation velocity.

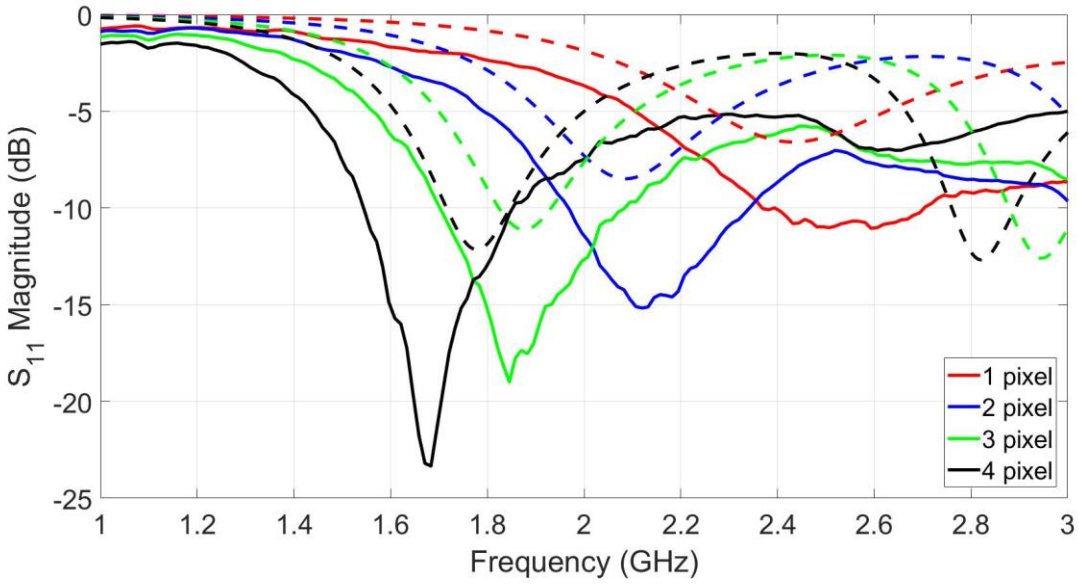

Figure 4.4: Measured data in comparison to a model simulated in HFSS. Simulated data shown in dashed line, measured data shown in solid line.

TABLE 0.1

Measured vs. Simulated Resonance Frequencies

'On' Pixels (per arm)	1	2	3	4
Measured (GHz)	2.51	2.12	1.85	1.68
Simulated (GHz)	2.43	2.08	1.88	1.78

The measured radiation patterns are that of a typical dipole antenna, with nulls at $\theta = 0°$ and 180° in the E-plane and an omnidirectional pattern in the H-plane (Figure 4.4). The variation in peak gain between the 1- and 4-pixel-per-arm cases is approximately ±3 dB. The cross-polarization ratio is between 10–20 dB.

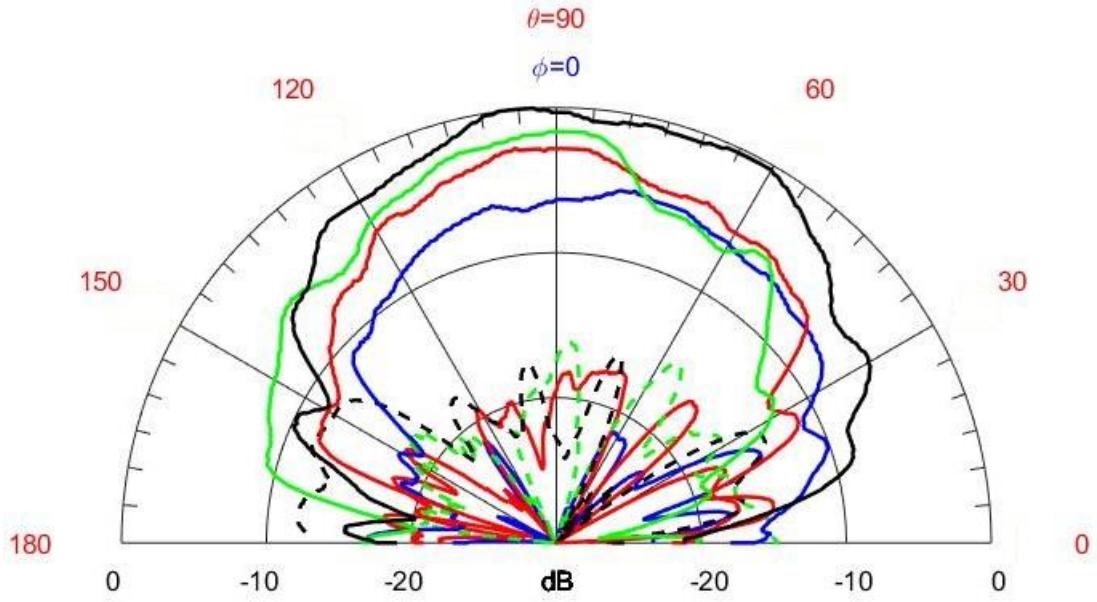

(a)

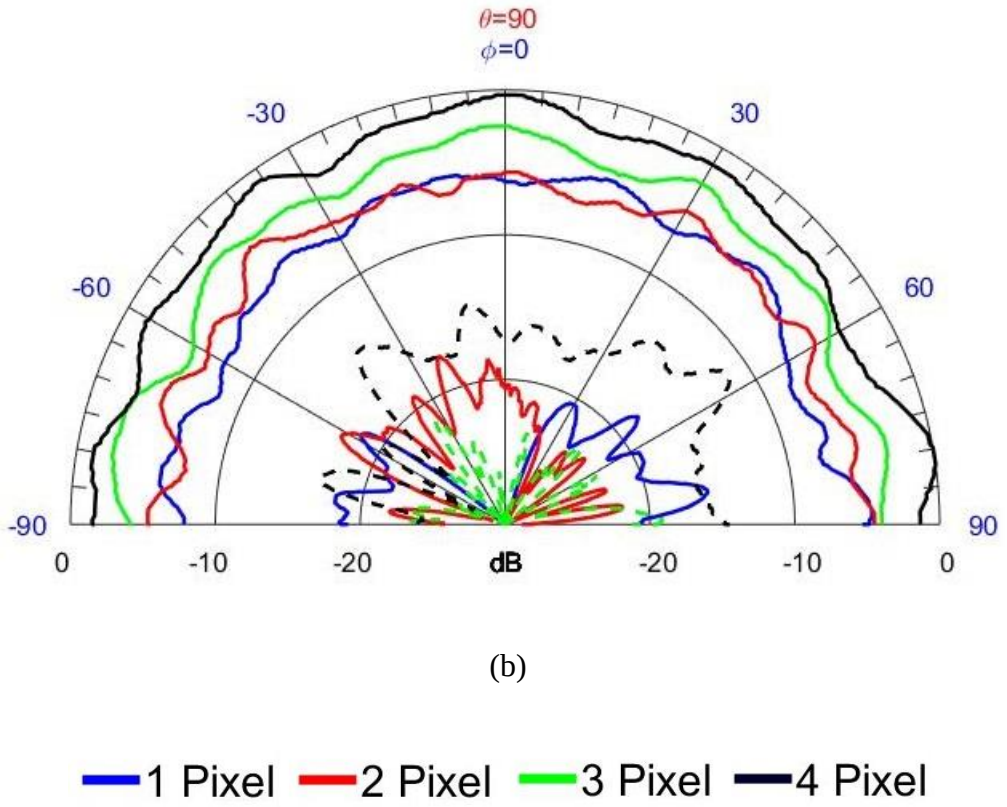

Figure 4.5: Measured co-polarized (solid) and cross-polarized (dashed) radiation patterns in the (a) E-plane and (b) H-plane.

The effect of pixelating the baseline dipole was also investigated. Figure 4.5 compares the measured radiation pattern of the baseline planar copper dipole to a pixelated copper equivalent. The pixelated copper antenna had a lower resonant frequency, but the effects of the shift were measured to be 2% and determined to be minimal. Frequency effects have been observed when replacing copper with liquid metal, but this was determined to be due to dielectric effects from the materials housing the liquid metal. Both antennas are tested at 2.1 GHz. This figure shows that pixelation of the dipole antenna presented in this chapter has negligible effects on the radiation pattern at the resonant frequency.

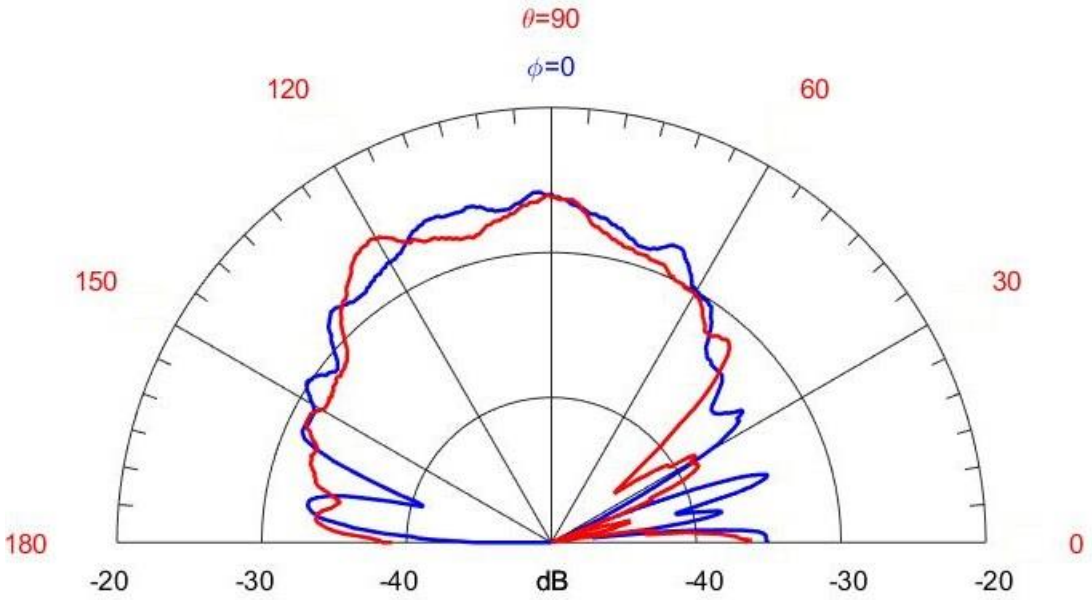
θ=90
ϕ=0
120
60
150
30
180
0
-20
-30
-40
dB
-40
-30
-20

(a)

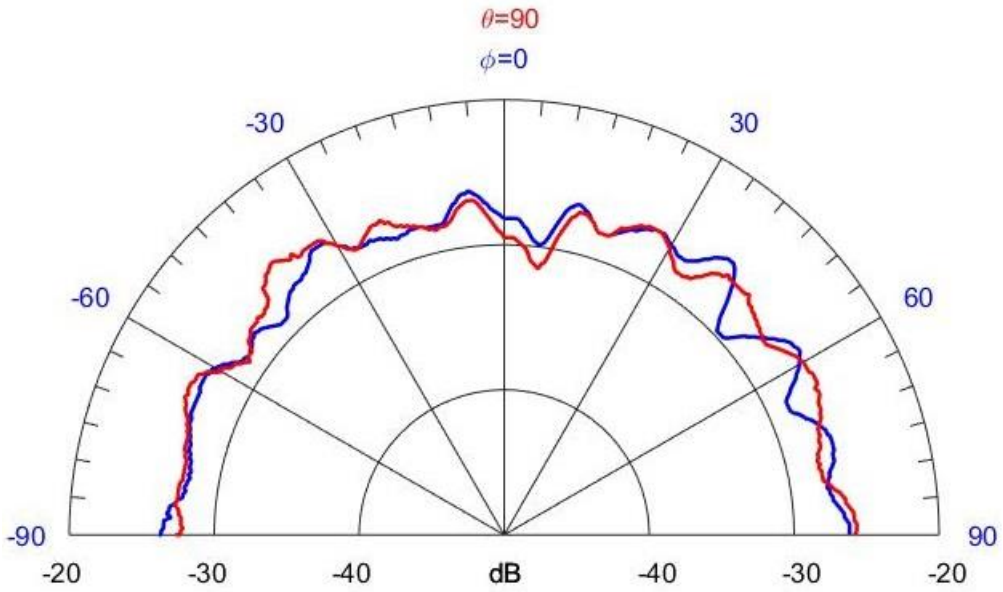
θ=90
ϕ=0
-30
30
-60
60
-90
90
-20
-30
-40
dB
-40
-30
-20

(b)

Figure 4.6: Comparison of baseline copper dipole and pixelated copper equivalent: (a) E-plane and (b) H-plane.

The gaps between pixels is limited to fabrication capabilities. Ideally, the gap is made as small as possible such that a continuous conductive surface is maintained. The gaps do influence antenna properties: charge tends to travel at the edge of the conductor that makes up the antenna. Any deformation in the edges, such as an indentation illustrated in Fig. 4.7, allow the antenna to be virtually longer, which lowers the operational frequency.

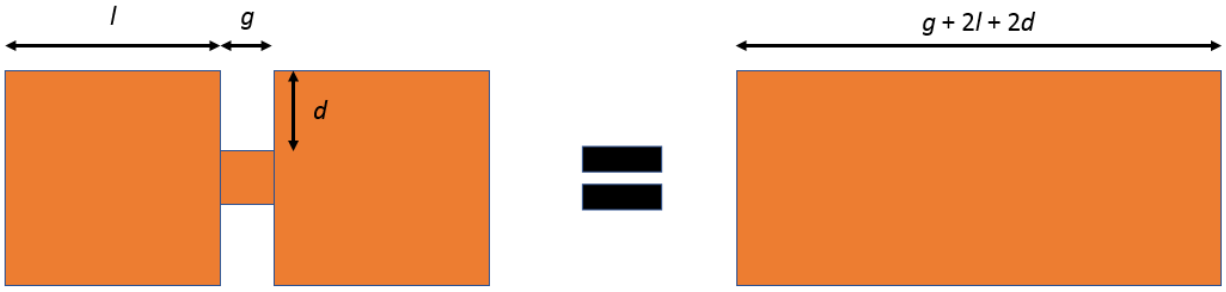

Figure 4.7: Effect of gap width between pixels: when two square conductors of length *l* are connected by a conductor of length *g*, current will travel along the edges of the square and connecting conductor, traveling a total distance of $g + 2l + 2d$.

4.5 Summary

This chapter demonstrates the first implementation of a pixelated antenna using liquid metal. Pixels actuate liquid metal with a 4-V signal to increase the length of a dipole antenna.

This allows a pixelated dipole antenna to resonate at 2.51 GHz, 2.12 GHz, 1.85 GHz, and 1.68 GHz. It has also been found that pixelation of the dipole antenna presented in this chapter has negligible effects on the radiation pattern at the resonant frequency

Conclusions and Future Work

This thesis has presented research and development of a liquid-metal pixel and its application to an antenna. By electrically actuating discrete amounts of liquid metal, a reconfigurable pixelated structure can be created to use as an antenna. This thesis investigated the ability for liquid metal to electrically actuate out-of-plane in Chapter 2, applied these findings to a pixelated architecture in Chapter 3 and applied the pixel to an antenna to achieve frequency reconfiguration in Chapter 4.

The ongoing research presented in this thesis has so far demonstrated frequency reconfiguration using pixels arrayed in one dimension. The next step is to demonstrate reconfiguration in two dimensions. Figure 5.1 below shows current developments for a liquid-metal dual-dipole antenna. This antenna aims to utilize liquid-metal pixels to switch between one dipole antenna to another that is rotated 90°. This would allow for the antenna to switch between vertical and horizontal polarization.

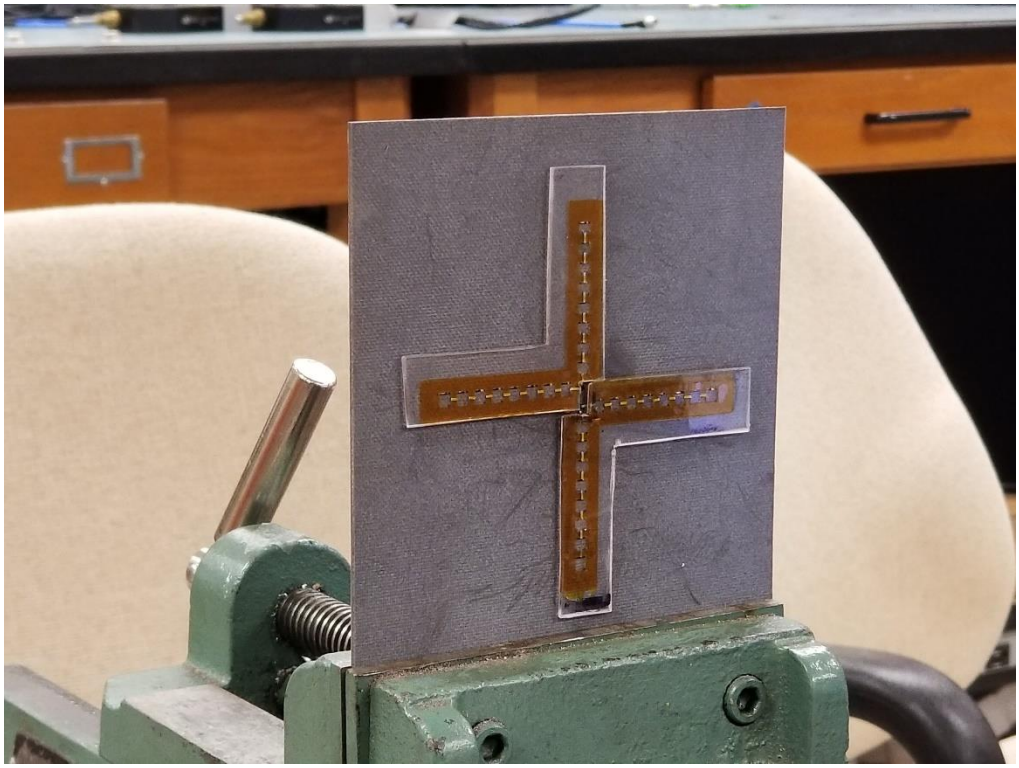

Figure 5.1: Prototype pixelated reconfigurable liquid-metal dual-dipole antenna

The long-term goal of the project is to utilize an $N \times N$ array that could realize N^2 possible permutations for use as an antenna. This would effectively allow users to draw out an antenna using software, like making a drawing on a computer monitor.

Bibliography

[1] Cell Phone Antenna Design [Online]. Available: http://www.antenna-theory.com/design/cellantenna.php, Accessed August 2016.

[2] C. G. Christodoulou, Y. Tawk, S. A. Lane, and S. R. Erwin, "Reconfigurable antennas for wireless and space applications," *Proc. IEEE,* vol. 100, no. 7, pp. 2250–2261, Apr. 2012.

[3] J. Constantine, Y. Tawk, S. E. Barbin, and C. G. Christodoulou, "Reconfigurable antennas: design and applications," *Proc. IEEE,* vol. 103, no. 3, pp. 424–437, Apr. 2015.

[4] S. Nikalaou, R. Bairavasubramanian, C. Lugo, I. Carrasquillo, D. C. Thompson, G. E. Ponchak, J. Papapolymerou, and M. M. Tentzeris, "Pattern and frequency reconfigurable annular slot using PIN diodes," *IEEE Trans. Antennas Propag.,* vol. 54, no. 2, pp. 439–447, Feb. 2006.

[5] N. Behdad and K. Sarabandi, "A varactor-tuned dual-band slot antenna," *IEEE Trans. Antennas and Propag.*, vol. 54, no. 2, pp. 401–408, Feb. 2006.

[6] E. Erdil, K. Topalli, M. Unlu, O. A. Civi, and T. Akin, "Frequency tunable patch antenna using RF MEMS technology," *IEEE Trans. Antennas and Propag.*, vol. 55, no. 4, pp. 1193–1196, Apr. 2007.

[7] A. M. Morishita, C. K. Y. Kitamura, A. T. Ohta, and W. A. Shiroma, "Two-octave tunable liquid-metal monopole antenna," *Electron. Lett.*, vol. 50, no. 1, pp. 19–20, Jan. 2014.

[8] M. Wang, M. R. Khan, C. Trlica, M. D. Dickey, and J. J. Adams, "Pump-free feedback control of a frequency reconfigurable liquid metal monopole," in *IEEE Int. Symp. on Antennas and Propag. & USNC/URSI National Radio Science Meeting,* Vancouver, BC, Canada, Oct. 2015, pp. 2223–2224.

[9] J.-H. So, J. Thelen, G. J. Hayes, G. Lazzi, and M. D. Dickey, "Reversibly deformable and mechanically tunable fluidic antennas," *Adv. Funct. Mater.,* vol. 19, no. 22, pp. 3632–3637, Sept. 2009.

[10] A. Ha and K. Kim, "Frequency tunable liquid metal planar inverted-F antenna," *Electron. Lett.*, vol. 52, no. 2, pp. 100–102, Jan. 2016.

[11] C. K. Y. Kitamura, A. M. Morishita, T. F. Chun, W. G. Tonaki, A. T. Ohta, and W. A. Shiroma, "A liquid-metal reconfigurable Yagi-Uda monopole array," in *IEEE MTT-S Int. Microw. Symp. Dig.*, Seattle, WA, USA, June 2013, pp. 1–3.

[12] D. Rodrigo, L. Jofre, and B. A. Cetiner, "Circular beam-steering reconfigurable antenna with liquid metal parasitics," *IEEE Trans. on Antennas and Propag.*, vol. 60, no. 4, pp 1796–1802, Feb. 2012.

[13] A. M. Morishita, C. K. Y. Kitamura, A. T. Ohta, and W. A. Shiroma, "A liquid-metal monopole array with tunable frequency, gain, and beam steering," *IEEE Antennas and Wireless Propag. Lett.*, vol. 12, pp. 1388–1391, Oct. 2013.

[14] M. R. Moorefield, R. C. Gough, A. M. Morishita, J. H. Dang, A. T. Ohta, and W. A. Shiroma, "Frequency-tunable patch antenna with liquid-metal-actuated loading slot," *Electron. Lett.*, vol. 52, no. 7, pp. 498–500, Mar. 2016.

[15] M. Kelley, C. Koo, H. Mcquilken, B. Lawrence, S. Li, A. Han, and G. Huff, "Frequency reconfigurable patch antenna using liquid metal as switching mechanism," *Electron. Lett.*, vol. 49, no. 22, pp. 1370–1371, Nov. 2013.

[16] R. C. Gough, J. H. Dang, A. M. Morishita, A. T. Ohta, and W. A. Shiroma, "Frequency-tunable slot antenna using continuous electrowetting of liquid metal," in *IEEE MTT-S Int. Microw. Symp. Dig.*, pp. 1–3, June 2014.

[17] D. Rodrigo and L. Jofre, "Frequency and radiation pattern reconfigurability of a multi-size pixel antenna," *IEEE Trans. Antennas Propag.*, vol. 60, no. 5, pp. 2219–2225, Mar. 2012.

[18] D. Rodrigo, B.A. Cetiner, and L. Jofre, "Frequency, radiation pattern and polarization reconfigurable antenna using a parasitic pixel layer," *IEEE Trans. Antennas Propag.*, vol. 62, no. 6, pp. 3422–3427, Mar. 2014.

[19] H. J. Lee, and C.-J. Kim, "Surface-tension-driven microactuation based on continuous electrowetting," *J. Microelectromech. Syst.*, vol. 9, no. 2, pp. 171–180, Jun. 2000

[20] J. Liu and X. Wang, "Recent advancements in liquid metal flexible printed electronics: properties, technologies, and applications," *Micromachines,* vol. 7, no. 12, Nov. 2016.

[21] M. D. Dickey, "Liquid metals for soft and stretchable electronics" in D.-H. Kim (Ed.), *Stretchable bioelectronics for medical devices and systems*, Switzerland, 2016, Springer International Publishing

[22] M. D. Dickey, "Emerging applications of liquid metals featuring surface oxides," *ACS Appl. Mater. Interface,* vol. 6, no. 21, pp. 18369–18379, Oct. 2014.

[23] J. H. Dang, R. C. Gough, A. M. Morishita, A. T. Ohta, and W. A. Shiroma, "Liquid-metal-based reconfigurable components for RF front ends," *IEEE Potentials*, vol. 34, no. 4, pp. 24–30, Jul. 2015.

[24] R. C. Gough, A. M. Morishita, J. H. Dang, M. R. Moorefield, W. A. Shiroma, A. T. Ohta, "Rapid electrocapillary deformation of liquid metal with reversible shape retention," *Micro and Nano Syst. Lett.*, vol. 3, no. 4, Dec. 2015.

[25] W. Irshad and D. Peroulis, "A 12–18 GHz electrostatically tunable liquid metal RF MEMS resonator with quality factor of 1400–1840," *IEEE MTT-S Int. Microw. Symp. Dig.*, Baltimore, Maryland, USA, June 2011, pp. 1-4

[26] Geratherm Medical AG: Galinstan Safety Data Sheet [online], Available: http://www.rgmd.com/msds/msds.pdf, Accessed August 2016.

[27] J. T. Bernhard, "Reconfigurable Antennas" in *Synthesis Lectures on Antennas,* London, U.K: Morgan & Claypool Publishers, 2007

[28] G. Mumcu, A. Dey, and T. Palomo, "Frequency-agile bandpass filters using liquid metal tunable broadside coupled split ring resonators," *IEEE Microw. Wirel. Compon. Lett.*, vol. 23, no. 4, pp. 187–189, Mar. 2013.

[29] R. C. Gough, J. H. Dang, A. M. Morishita, A. T. Ohta. and W. A. Shiroma, "Reconfigurable coupled-line bandpass filter with electrically actuated liquid-metal tuning," *Asia-Pacific Microwave Conf.,* Sendai, Japan, Nov. 2014, pp. 932–934

[30] M. Li, and N. Behdad, "Fluidically tunable frequency selective/phase shifting surfaces for high-power microwave applications," *IEEE Trans. Antennas Propag.,* vol. 60, no. 6, pp. 2748–2759, Apr. 2012.

[31] J. H. Dang, R. C. Gough, A. M. Morishita, A. T. Ohta, and W. A. Shiroma, "Liquid-metal-based phase shifter with reconfigurable EBG filling factor," *IEEE MTT-S Int. Microwave Symp. Dig.,* Phoenix, AZ, May 2015, pp. 1–4.

[32] K. J. Sarabia, S. S. Yamada, R. C. Gough, M. R. Moorefield, A. W. Combs, W. A. Shiroma, and A. T. Ohta, "Out-of-plane continuous electrowetting of liquid metal," *Electron. Lett.,* Oct. 2017.

[33] C. G. Christodoulou, L. F. Feldner, V. Zachou, and D. Anagnostou, "Planar reconfigurable antennas," in *2006 First European Conference on Antennas and Propagation,* Nice, France, pp. 1–7, Nov. 2006.

[34] A. G. Besoli, and F. De Flavii, "A multifunctional reconfigurable pixels antenna using MEMS technology on printed circuit board," *IEEE Trans. Antennas Propag.*, vol. 60, no. 12, pp. 4413–4424, Aug. 2011.